https://doi.org/10.5194/acp-2022-778
Preprint. Discussion started: 14 December 2022

Atmospheric Chemistry and Physics
Discussions

On the Quasi-2-Day Planetary Waves in the Middle Atmosphere During Different QBO Phases

Liang Tang[1], Sheng-Yang Gu[2*], Shu-Yue Zhao[2], Dong Wang[2]

[1] School of Optoelectronic Engineering, Chongqing University of Posts and Telecommunications, Chongqing, China.

[2] Electronic Information School, Wuhan University, Wuhan, China.

*Corresponding author: Sheng-Yang Gu, (gushengyang@whu.edu.cn)

https://doi.org/10.5194/acp-2022-778
Preprint. Discussion started: 14 December 2022

Atmospheric Chemistry and Physics
Discussions

Abstract. We found that the interannual difference of the W3 and W4 Q2DW is significantly correlated with the Quasi-Biennial Oscillation westerly (QBOW) and easterly (QBOE) phase, identified from the analysis of the 2003 to 2020 MERRA-2 and SABER atmospheric data. The amplitude of the zonal wind in the QBOE phase is approximately ~10 m/s stronger than that in the QBOW phase. Mean zonal easterly winds are stronger in the QBOE phase than in the QBOW phase, while westerly winds are stronger in the QBOW phase. The Q2DW is present in the summer, and the background wind is easterly in both hemispheres. The mean temperature amplitudes of W3 and W4 in the QBOW phase are stronger than those in the QBOE phase, and the difference is ~2 K and ~3 K (in the Southern Hemisphere); ~2 K and ~3 K (in the Northern Hemisphere), respectively. The mean wave period of W4 in the QBOW phase in the Northern Hemisphere is shorter than that in the QBOE phase. The W3 mode is modulated by atmospheric eigenmodes in both hemispheres and shows slight differences in the QBOW and QBOE phases, while the W4 mode is more likely to show significant differences in the different QBO phases. Our diagnostic analysis suggests that the amplification of the QBOW phases W3 and W4 may be due to stronger mean-flow instabilities and background winds in the mesosphere. In addition, planetary waves gain stronger source activity during the QBOW phase to provide sufficient energy for propagation and amplification.

https://doi.org/10.5194/acp-2022-778
Preprint. Discussion started: 14 December 2022

Atmospheric Chemistry and Physics Discussions

1 Introduction

The Quasi-Biennial Oscillation (QBO) is the most prominent feature of the equatorial stratospheric circulation (Holton and Tan, 1980; Holton and Austin, 1991). Since 1953, weakening easterly and westerly winds have been observed in the lower tropical stratosphere for approximately 28 months (Baldwin et al., 2001; Naujokat, 1986; Veryard and Ebdon, 1961; Reed et al., 1961). The QBO is sustained mainly by large-scale Kelvin waves, Rossby gravity, gravity waves, and momentum deposits from vertical advection. The latitude range of QBO observation is 15°N-15°S. The influence of QBO on the tropical stratosphere and the tropical troposphere has been well known, for example, the Hadley circulation (Gray et al., 1992; Zhang et al., 2022; Jiang et al., 2022; Sun et al., 2022; Reid et al., 2022) and the Madden–Julian Oscillation (Yoo and Son, 2016; Son et al., 2017; Marshall et al., 2017; Nishimoto and Yoden, 2017; Hood et al., 2020; Martin et al., 2019). Nao et al. (2010) and Yamashita et al. (2011) indicate the secondary circulation caused by equatorial QBO is important in the middle stratosphere, but not in the lower stratosphere. Peña-Ortiz et al. (2019) studied the effect of QBO on tropical convection and revealed the regulating effect of QBO on tropical convection. They found that tropical convection influences stationary waves and polar vortices in the southern hemisphere during winter. Lu et al. (2014) and Garfinkel et al. (2012) consider the significance of the meridional circulation anomaly caused by QBO extending from subtropical to mid-latitude through the change of refractive index and the modulation of Rossby wave propagation.

The QBO impacts the extratropical stratosphere by modulating the strength of the stratospheric polar vortex (Gray et al., 2004; Baldwin et al., 2001; Holton and Austin, 1991; Holton and Tan, 1980). Tian et al. (2019) believe that QBO has a greater influence on the interannual tropical water vapor anomalies than El Niño–Southern Oscillation (ENSO) in the middle and lower stratosphere. For the westerly phase of the QBO (QBOW), the tropical water vapor interannual anomaly is positive near the tropopause and in the lower stratosphere, negative in the middle stratosphere, and positive in the upper stratosphere. Vice versa for the easterly phase of the QBO (QBOE). Ma et al. (2021) found that the East Asian winter monsoon in the early winter months is weaker in the QBOE than in the QBOW during 1958–2019. In addition, they found that the activity of planetary waves also changes in association with the QBO. Their examination of the zonal wavenumbers (WNs) of planetary waves in the sea level pressure (SLP) field shows that WN1 strengthened and WN 2 and WN 3 weakened during QBOE.

Yamazaki et al. (2020) propose that the tropospheric anomaly generates a Rossby wave train that propagates into the mid-latitude troposphere and interferes with stationary waves, especially with

https://doi.org/10.5194/acp-2022-778
Preprint. Discussion started: 14 December 2022

wavenumber 1, resulting in enhanced upward planetary wave propagation and weakened polar vortex. Based on the modulation of the 11-year solar cycle, they concluded that the QBO (QBOE-QBOW) in outgoing longwave radiation (OLR) was strong in the solar min years with significantly enhanced convection over the western tropical Pacific. Li et al. (2020) demonstrated for the first time that the synoptic Rossby waves enhanced at ~40 hPa in the tropics in February 2016 came from both the extratropical and the local wave generation. They suggest that the forcing of the unusually long-lasting westerly zonal phase in the middle stratosphere (~20 hPa), is mainly caused by the enhanced Kelvin wave activity. Lu et al. (2019) found that the interannual variation of ~2-5 days eastward propagating planetary waves was positively correlated with zonal-mean zonal winds averaged over 67.5°±10°S, but negatively correlated with the QBO index in the southern winter. In addition, they believe that the growth rate (stronger wave) of eastward propagating planetary waves generated by strong polar night jet (PNJ) is greater in QBOE than in QBOW phase, explaining the QBO-like signal in Antarctic planetary waves.

The short-period (~2–16 days) planetary Rossby waves propagate westward relative to the ground, which is primarily caused by the uneven distribution of sea-land topography and atmospheric temperature. Planetary waves cause significant perturbations and diurnal variability in

https://doi.org/10.5194/acp-2022-778
Preprint. Discussion started: 14 December 2022

the dynamics, chemistry, and composition of the mid-latitude stratosphere and mesosphere (Qin et al., 2021b; Qin et al., 2021a; Iimura et al., 2021; Liu et al., 2020; Liu et al., 2019; Xiong et al., 2018; Pancheva et al., 2018). Quasi-2-day waves (Q2DWs) play an important role in planetary wave observation because of their shorter period and stronger amplitude (Iimura et al., 2021; Gu et al., 2021; Gu et al., 2019; Pancheva et al., 2018; Kumar et al., 2018; Gu et al., 2018; Ma et al., 2017; Pancheva et al., 2016). Previous literature studies mainly focused on the observation of Q2DW with zonal wavenumbers 2 (W2), 3 (W3), and 4 (W4). The amplitude of Q2DW W3 is the strongest among the three modes in the Southern Hemisphere (SH), and W4 is relatively strong in the Northern Hemisphere (NH). The amplitude of W2 is relatively weaker than that of W3 and W4 in both hemispheres, but it can nevertheless be measured by space-based detectors. The propagation and amplification of Q2DWs are closely related to a theory of normal modes. (Salby, 1981a; Salby, 1981b) believed that W3 and W4 were Rossby-gravity wave modes (3, 0) and (4, 0), respectively, in the real atmosphere, which could modulate and extract energy through the background mean flow. However, Plumb et al. (1983) suggested that the amplification and propagation of Q2DWs might be the result of the barotropic/baroclinic instability in the middle-high latitudes of the summer hemisphere. Previous studies have extensively discussed the mechanism of dual propagation and amplification of Q2DWs. Q2DWs are usually

https://doi.org/10.5194/acp-2022-778
Preprint. Discussion started: 14 December 2022

defined as having the characteristics of normal modes while being amplified due to barotropic/baroclinic instabilities.

The WACCM + data assimilation research method was proposed by (Gu et al., 2016). They found that the largest Q2DWs amplitudes in the SH during 2007 occurred in early Jan (W2), late Jan (W3), and late Feb (W4), respectively, and indicated that background conditions in these three periods favored the propagation and amplification of these three modes. Mccormack et al. (2014) used the data assimilation system from the NOGAPS-ALPHA during 2007-2009 to find the changes between Q2DWs and migrating diurnal tides. In addition, the short-term variation of migrating diurnal tides may be caused by the nonlinear interaction between tidal waves and Q2DWs (Chang et al., 2011). Gu et al. (2021) found that W3 and W4 occurred more frequently around 48 h, while W2 tended to be short-period events. In addition, they found that the wave periods of W3 and W4 rise during the late summer in the Northern Hemisphere. Tang et al. (2021) found the eastward wave in winter periods and westward background wind in both hemispheres. In addition, they observed that the mean phase speeds of zonal wavenumbers -1 (E1), -2 (E2), -3 (E3), and -4 (E4) were relatively stable, which are ~53 m/s, ~58 m/s, ~55 m/s, and ~52 m/s, respectively, at 70° latitude. Their diagnostic analysis suggests that mean-flow instabilities in the upper stratosphere and mesosphere may be responsible for the amplification of PWs.

https://doi.org/10.5194/acp-2022-778
Preprint. Discussion started: 14 December 2022

Previous works have independently investigated anomalous phenomena of QBO and perturbations of atmospheric circulation and monsoons, and studies of planetary waves have focused more on variable wave properties. Few previous studies have explored the relationship between QBO and planetary waves in detail. Therefore, the present study focuses on exploring the QBOE/QBOW contributions to W4 and W3 during the 2003-2020 summer.

In this study, we use the Thermosphere, Ionosphere, Mesosphere, Energetics, and Dynamics (TIMED) satellite and the second modern retrospective research and application analysis (MERRA-2) datasets to investigate the contribution of QBO to W3 and W4 westward propagating waves in the mesosphere during the 2003-2020 summer period. Specifically, we investigate the distribution of W3 and W4 in QBOE and QBOW, as well as the variability of planetary waves in different phases; Also, the role of instabilities, background wind structure, and critical layers in propagation and amplification. The remainder of the paper is structured as follows. In Sec. 2, two kinds of datasets and diagnostic analysis and planetary wave fitting methods used in our study are introduced: the SABER datasets used to observe Q2DWs, the datasets required for diagnostic analysis (MERRA2), and the method of diagnostic analysis. In Sec. 3, we explore the differences between W4 and W3 events during the 2003 to 2022 QBOW and QBOE phases, including the mean temperature

https://doi.org/10.5194/acp-2022-778
Preprint. Discussion started: 14 December 2022

structure, instabilities, and background winds, and reveal the mechanism of W3 and W4 propagation and amplification in QBOW and QBOE phases. Sec. 4 provides a summary and conclusions.

2 Datasets and Analysis Method

The long-term Sounding of the Atmosphere using Broadband Emission Radiometry (SABER) observations located on the TIMED satellite was launched in July 2001 with the mission of studying the human influence on the least detected and recognized regions of Earth's atmosphere: the mesosphere, lower thermosphere, and ionosphere (MLTI). The SABER data set is optimal for studying the variability of Q2DWs, as they completely cover the vertical region of the mid-atmosphere where the waves are strongest. The SABER temperature data focuses on a region of approximately 20 to 120 km, with vertical and latitude resolutions of 4km and 4°, respectively. In addition, the combined effects of random and systematic errors in the lower and middle stratosphere are ~1.4 K and ~1 K, respectively (Remsberg et al., 2008). The SABER sampling has two positions of ~50°S-80°N and ~80°S-50°N, changing every ~60 days. These data are widely used to study the mid-atmosphere, such as planetary waves, tidal waves, and climate variability in the mesosphere and lower thermosphere (Lu et al., 2019; Liu et al., 2019; Gu et al., 2019; Gu et al., 2018; Huang et al., 2013). These studies suggest that the TMED/SABER data are plausible and therefore appropriate for our investigation. The

https://doi.org/10.5194/acp-2022-778
Preprint. Discussion started: 14 December 2022

Q2DW events were extracted from the temperature data measured by SABER from 2002 to 2020, were observed at ~30-40°(S/N) and ~67-73 km for W4, and ~30-40°S and ~79-85 km; ~30-40°N and ~67-73 km for W3.

The Second Modern Era-Retrospective Analysis for Research and Applications (MERRA-2) reanalysis data (Gelaro et al., 2017) are used to provide a background environment from the surface to the top boundary of ~80 km for characterizing the Q2DWs. So far, MERRA-2 produced real QBO in zonal winds, mean meridional circulation, and ozone (Coy et al., 2016). The temporal resolution (~1 h), vertical resolution (~2-3 km), and spatial resolution (~0.5*0.625) of MERRA-2 data were fixed. The MERRA-2 data have numerous applications in polar atmospheres, planetary waves, climate change rates, atmospheric circulation, etc. These studies validate the authenticity of the MERRA-2 data. The long-term MERRA-2 data from 2003 to 2020 were used to diagnose the contribution of QBO with different phases to W3 and W4 during the summer and to analyze background winds, instabilities, source activity, and critical layer variability.

A least-squares fitting method was used to fit the SABER temperature observations and extract W3 and W4 for the summer period. In our analysis, we use a temporal window of ~6 days to analyze the fluctuations of the period from ~36 to ~60 h in a step of ~2 h. We extract the maximum

https://doi.org/10.5194/acp-2022-778
Preprint. Discussion started: 14 December 2022

amplitude and the corresponding period from the analysis window.

$$y = A\cos[2\pi(\sigma \cdot t + s \cdot \lambda)] + B\sin[2\pi(\sigma \cdot t + s \cdot \lambda)] + C \quad (1)$$

The amplitude of a planetary wave can be defined as $R = \sqrt{A^2 + B^2}$. The fitted parameter variables are A, B, and C in Formula (1), respectively. The planetary wave frequency and zonal wavenumber correspond to σ and s, respectively. The UT time and longitude of the satellite sample are t and λ respectively. C denotes a zonal mean temperature.

Planetary waves in the lower atmosphere are absorbed or reflected by the critical layer as they propagate upwards. Planetary waves that gain sufficient energy in the unstable region are amplified by reflection. In other words, the critical layer has an important effect on the amplification and propagation of planetary waves (Liu et al., 2004). In the critical layer, the phase speed (c) is equal to the background zonal wind ($\bar{u}$).

$$\overline{q_\varphi} = 2\Omega\cos\varphi - \left(\frac{(\bar{u}\cos\varphi)_\varphi}{a\cos\varphi}\right)_\varphi - \frac{a}{\rho}\left(\frac{f^2}{N^2}\rho\bar{u}_z\right)_z \quad (2)$$

In the spatial structure of the atmosphere, barotropic/baroclinic instability may occur in regions with negative latitudinal gradients and quasigeostrophic potential vorticity ($\overline{q_\varphi}$). Previous studies have shown that instability contributes to the amplification and propagation of planetary waves.

In Equation (2), the Coriolis parameter, Earth radius, and background air density correspond to f, a and ρ, respectively; Ω is the angular

https://doi.org/10.5194/acp-2022-778
Preprint. Discussion started: 14 December 2022

Atmospheric Chemistry and Physics Discussions

speed of the Earth's rotation; $\bar{u}$ is the zonal mean zonal wind; φ is the latitude; N is the buoyancy frequency; subscripts z and φ are the vertical and latitudinal gradients.

3 Results and Discussion

Figure 1a confirms that the amplitude of mean zonal winds at 40 hPa above the equator from 2003 to 2020 varies from -20m/s (easterly) to 20 m/s (westerly), obtained from MERRA-2, as shown by periodic changes in phase with intervals of ~28 months. In Figure 1b, the blue line represents the QBO index (latitude 0 and 40 hPa), obtained from MERRA-2, the red shade is the zonal wind -5 m/s to 5 m/s, and ° and * represent the W3 and W4 events. Red for the southern hemisphere and green for the northern. Annual mean zonal wind variability can be found, with anomalous zonal wind variability in the QBO in 2010, 2012, 2016, and 2018. The maximum amplitude of the 2010 zonal wind reaches ~-29 m/s, which is close to the maximum in the QBOE phase. The amplitude of the zonal wind is significantly stronger in the QBOE phase than in the QBOW phase, reaching ~-25 m/s and ~15 m/s, respectively.

Dates of W3 and W4 Q2DW events from 2003 to 2020, obtained with SABER. The southern hemisphere W3 observations were extracted from ~79-85 km and ~30-40°S; W4 is extracted from ~67-73 km and ~30-40°S. The northern hemisphere W3 and W4 observations were extracted from ~67-73 km and ~30-40°N. We mainly study the Q2DW difference between

https://doi.org/10.5194/acp-2022-778
Preprint. Discussion started: 14 December 2022

QBOW and QBOE phases, so the following analysis will eliminate the events with insignificant phase changes (red shading). The W3 and W4 events in the QBOW phase of the Southern Hemisphere summer were found to be distributed in 2003, 2005, 2007, 2009, 2011, 2014, and 2017. The W3 and W4 events in the QBOE phase were distributed in 2004, 2006, 2008, 2013, and 2015. Similarly, W3 and W4 events in the QBOW phase during the Northern Hemisphere summer were distributed in 2004, 2006, 2008, 2009, 2011, 2013, 2017, and 2019. In the QBOE phase, W3 and W4 events are assigned to the years 2003, 2005, 2007, 2010, 2012, 2015, 2016, 2018, and 2020.

Figure 2 shows the seasonal variation of QBOW and QBOE mean zonal wind at 70°(S/N), obtained from MERRA-2, and the QBOW-QBOE difference from 2003 to 2020. Figures 2a and 2c show that the background means zonal winds in the Southern Hemisphere are easterly in summer and westerly in winter, with the maximum westerly fluctuations being lower and stronger than the easterly ones. During the QBOW phase, mean zonal winds in the Southern Hemisphere reach maximum easterly winds of ~-40 m/s at ~70 km in late December-early January. In August-September, westerly winds at ~50 km reach ~75 m/s. Similarly, in the QBOE phase, the maximum easterly wind at ~70 km reaches ~-42 m/s from late December to early January, and the maximum westerly wind at ~50 km reaches ~66 m/s from late August to early September. Figure 2e shows the

https://doi.org/10.5194/acp-2022-778
Preprint. Discussion started: 14 December 2022

difference between QBOW and QBOE in the Southern Hemisphere. The QBOE has stronger easterly winds at 60-80 km than the QBOW in summer, with a maximum difference of ~3 m/s. Westerly winds are stronger in the QBOW than in the QBOE at ~40-60 km in winter, with a maximum difference of ~22 m/s.

Similarly, Figures 2b and 2d show that the background means zonal winds in the Northern Hemisphere are westerly in winter and easterly in summer. Mean zonal winds in the QBOW phase reach maximum westerly winds of ~58 m/s at ~70 km in December and easterly winds of ~-42 m/s at ~70 km in late June-early July. Similarly, the maximum westerly wind at ~50 km during the QBOE phase in early January reaches ~46 m/s, and the maximum easterly wind at ~70 km in July reaches ~-43 m/s. Figure 2f shows the difference between QBOW and QBOE in the Northern Hemisphere. QBOW has stronger westerly winds at ~40-80 km in winter than QBOE, with a maximum difference of ~42 m/s, while QBOE has stronger westerly winds at ~20-60 km in winter around Jan, with a difference of ~30 m/s. Easterly winds at ~60-80 km are stronger in the QBOE than in the QBOW during the summer months, with a maximum difference of ~2 m/s.

Figure 3 shows the spectral and temperature spatial structure of W3 and W4 in the 2006 and 2007 QBOW and QBOE phases, and the difference in their spatial structure in the QBOW and QBOE phases. Figure 3A1-3A2

https://doi.org/10.5194/acp-2022-778
Preprint. Discussion started: 14 December 2022

(3B1-3B2) and 3A3-3A4 (3B3-3B4) show the event analysis of the 2006 QBOE and 2007 QBOW phases of W3 (W4) in the Southern Hemisphere. Figure 3A1 shows the least-squares fitted spectra of SABER temperature of QBOE phase W3 at ~80 km and ~30-40°S during 13-19 days 2006. The wavenumber 3 signal with a period of ~43 h is distinctly dominant throughout the spectrum. Figure 3A2 shows the corresponding temperature space structure. The temperature spatial structure of W3 reaches a maximum of ~17 K at ~30-40˚S and ~82 km, and the remaining reaches a maximum of ~12 K (~68 km). Similarly, Figure. 3A3, the spectrum of W3 in QBOW phase is observed at ~80 km and ~30-40°S on 21-27 days 2007, when wavenumber 3 becomes the main wave mode and the wave period, is ~52 h. Figure 3A4 shows that the temperature spatial structure of W3 reaches a maximum of ~14 K at ~30-40˚S and ~82 km. Figure 4A5 shows that the temperature amplitude of W3 is weaker in the QBOW phase than in the QBOE phase, with the maximum difference reaching ~7 K. Figure 3B1 shows the observed spectra of W4 in QBOE at ~70 km and ~30-40°S at 45-51 days 2006, and the wave period of locked wavenumber 4 is ~65 h. Figure 3B2 shows that the temperature spatial structure of W4 is ~2 K at ~30-40˚S and ~68 km. Similarly, Figure. 3B3, the spectrum of W4 in QBOW phase is observed at ~70 km and ~30-40°S on 41-47 days 2007, when wavenumber 3 becomes the main wave mode and wave period is ~49 h. Figure 3B4 shows that the temperature spatial structure of W4 reaches a

https://doi.org/10.5194/acp-2022-778
Preprint. Discussion started: 14 December 2022

maximum of ~4 K at ~30-40˚S and ~68 km. Figure 4B5 shows that the W4 temperature amplitude is stronger in the QBOW phase than in the QBOE phase, with the maximum difference reaching ~3 K.

Figure 3C1-3C2 (3D1-3D2), and 3C3-3C4 (3D3-3D4), show the 2006 QBOW and 2007 QBOE phase events of W3 (W4) in the Northern Hemisphere. Figure 3C1 shows the 194-200 days 2006 spectrum of W3 at ~70 km and ~30-40°N in the QBOW phase. The wavenumber 3 signal with a period of ~47 h is distinctly dominant throughout the spectrum. As shown in Figure 3C2, the temperature spatial structure of W3 reaches a maximum value of ~7 K at ~30-40˚N and ~82 km, and another value of ~6 K (~68 km). Similarly, Figure. 3C3, the spectrum of W3 in the QBOE phase is observed at ~70 km and ~30-40°N on 198-204 days 2007, when wavenumber 3 becomes the main wave mode and wave period is ~53 h. Figure 3C4 shows that the temperature spatial structure of W3 reaches a maximum of ~6 K at ~30-40˚N and ~68 km. Figure 4C5 shows that the W3 temperature amplitude is stronger in the QBOW phase than in the QBOE phase, with the maximum difference reaching ~2 K. Figure 3D1 shows the observed spectra of W4 in QBOW at ~70 km and ~30-40°N at 210-216 days 2006, with a wave period of ~47 h for locked wavenumber 4. Figure 3D2 shows that the temperature spatial structure of W4 is ~10 K (~8 K) at ~30-40˚N and ~68 km (~82 km), respectively. Similarly, in Figure 3D3, the spectrum of W4 in the QBOE phase is observed at ~70 km and ~30-40°N

https://doi.org/10.5194/acp-2022-778
Preprint. Discussion started: 14 December 2022

on 180-186 days 2007, when the wavenumber 4 becomes the main wave mode and the wave period is ~49 h. Figure 3D4 shows that the temperature spatial structure of W4 reaches a maximum of ~6 K at ~30-40˚N and ~68 km. Figure 4D5 shows that the W4 temperature amplitude in the QBOW phase is almost two times stronger than that in the QBOE phase, with the maximum difference reaching ~7 K.

3.1 In the Southern Hemisphere

Spatial structure of mean temperature extracted from events W3 and W4 in the Southern Hemisphere QBOW and QBOE phases from 2003 to 2020 (see Figure 4). As shown in Figure 4a, the mean temperature spatial structure of W3 in the QBOW phase has two peak amplitudes at ~68 km and ~82 km at 30-40˚S, which are ~8 K and ~13 K respectively. The spatial structure of W3 in the QBOE phase also has a bimodal structure with maximum fluctuations at ~30-40˚S and ~82 km with an amplitude of ~12 K (Figure 4b). The other peak is at ~68 km, at ~8 K. Figure 4c shows the difference of W3 in the QBOW and QBOE phases. It is clear that the temperature amplitude of W3 is stronger in the QBOW phase at ~30-40˚S and ~70-90 km than in the QBOE phase, and the maximum difference reaches ~2 K.

Similarly, the mean temperature spatial structure of W4 in the QBOW phase has two peaks at ~30-40˚S with amplitudes of ~68 km and ~82 km at ~5 K and ~4 K, respectively (Figure 4d). As shown in Figure 4e, the

https://doi.org/10.5194/acp-2022-778
Preprint. Discussion started: 14 December 2022

fluctuation amplitude of W4 in the QBOE phase is ~2 K at ~30-40°S and ~70 km (~82 km). Figure 4f shows the difference between W4 in the QBOW and QBOE phases. It is clear that the temperature amplitude of W4 in the QBOW phase at ~25-50°S and ~65-90 km is stronger than that in the QBOE phase, being nearly twice as strong, and the maximum difference reaches ~3 K.

Figures 5a and 5b show the results of the diagnostic analysis for W3 events in the QBOW and QBOE phases, respectively. W3 in the QBOW is more favorable for dispersal during the Southern Hemisphere summer, largely amplified by the mean flow instability between 40-60°S and ~70-80 km and the appropriate background winds. In addition, the wave-mean flow interaction near the critical layer (~48 h) of the green curve is conducive to the propagation and amplification of W3 (Figure 5a). As shown in Figure 5b, wave-mean flow interactions of W3 in the QBOE near the critical layer of the green curve (~47 h) and instability and background winds in the range of ~40-60°S and ~70-80 km provide energy for propagation and amplification. It can be found that the background winds and instabilities of W3 are stronger in the QBOE phase than in the QBOW phase. Figures 5c and 5d illustrate the diagnostic analysis of W4 at the QBOW and QBOE phases, respectively. It is more likely that W4 in QBOW propagates during the Southern Hemisphere summer, with mean-flow instabilities and background winds providing sufficient energy to

Atmospheric Chemistry and Physics Discussions

significantly propagate and amplify W4 at mid-high latitudes and ~70-80 km. In addition, W4 is amplified and propagated by wave-mean flow interactions near the critical layer (~52 h) of the green curve (Figure 5c). As shown in Figure 5d, the instability and background wind of W4 in the QBOE at ~40-60˚S and ~70-80 km, as well as wave-mean flow interactions near the critical layer of the green curve (~51 h), provide energy for propagation and amplification. The instability of W3 and the background wind is weaker in the QBOW phase than in the QBOE phase, which is inconsistent with the spatial structure result. We suspect that the Southern Hemisphere W3 mode is mainly affected by the atmospheric eigenmodes and that the difference between the mean temperature amplitudes in the QBOW and QBOE phases is small. However, the W4 instabilities and background winds are stronger in the QBOW phase than in the QBOE phase, in agreement with the spatial structure results.

3.2 In the Northern Hemisphere

Spatial structure of mean temperature extracted from W3 and W4 events during the Northern Hemisphere QBOW and QBOE phases from 2003 to 2020 (see Figure 6). As shown in Figure. 6a, the mean temperature spatial structure of W3 in the QBOW phase has two peak amplitudes at ~68 km and ~82 km of 30-40˚N, which are ~6 K and ~6 K, respectively. The spatial structure of W3 in the QBOE phase is unimodal, with the largest fluctuation at ~30-40˚N and ~68 km, with an amplitude of ~4 K

https://doi.org/10.5194/acp-2022-778
Preprint. Discussion started: 14 December 2022

(Figure 6b). Figure 6c shows the difference between W3 in the QBOW and QBOE phases. The results show that the temperature amplitude of the QBOW phase of W3 at ~30-40˚N and ~70-90 km is stronger than that of the QBOE phase, and the maximum difference reaches ~2 K. As shown in Figure 6d, the mean temperature spatial structure of W4 in the QBOW phase has two peaks at ~30-40 ˚N, with amplitudes of ~68 km and ~82 km at ~7 K and ~4 K, respectively. As shown in Figure 6e, the fluctuation amplitude of W4 in the QBOE phase is ~5 K (~ 4K) at ~30-40˚N and ~68 km (~82 km). Figure 6f shows the difference between W4 in the QBOW and QBOE phases. It can be seen that the temperature amplitudes of W4 at ~30-40˚N and ~65-90 km of the QBOW phase are nearly twice stronger as those of the QBOE phase, and the maximum difference reaches ~3 K.

Figures 7a and 7b show the results of the diagnostic analysis for W3 events in the QBOW and QBOE phases, respectively. W3 in the QBOW is more conducive to propagation and amplification in the Northern Hemisphere summer due to mean flow instability between 40 and 60˚N and 70 to 80 km and appropriate background winds. In addition, the wave-mean flow interaction near the critical layer of the green curve (~51 h) is favorable for W3 propagation and amplification (Figure 7a). As shown in Figure 7b, wave-mean flow interactions of W3 in the QBOE near the critical layer of the green curve (~51 h) and instability and background winds in the range of ~40-60˚N and ~70-80 km provide energy for

https://doi.org/10.5194/acp-2022-778
Preprint. Discussion started: 14 December 2022

Atmospheric Chemistry and Physics Discussions
Open Access

propagation and amplification. It can be found that the background winds and instabilities of W3 are stronger in the QBOW phase than in the QBOE phase. Figures 7c and 7d show the diagnostic analysis of W4 at the QBOW and QBOE phases, respectively. W4 in QBOW is more likely to propagate during the Northern Hemisphere summer months, as mean-flow instabilities and background winds at mid-latitudes and ~70-80 km provide sufficient energy to significantly enhance W4 propagation and amplification. In addition, W4 is amplified and propagated by wave-mean interactions near the critical layer (~43 h) of the green curve (Figure 7c). As shown in Figure 7d, the instability and background wind of W4 in the QBOE at ~40-60°N and ~70-80 km, as well as wave-mean flow interactions near the critical layer of the green curve (~47 h), provide energy for propagation and amplification. It can be seen that the instability of W3 and the background wind is stronger in the QBOW phase than in the QBOE phase, which is consistent with the spatial structure results. Similarly, the W4 instabilities and background winds are stronger in the QBOW phase than in the QBOE phase, in agreement with the spatial structure results. We suspect that the differences between the mean temperature amplitudes of the W3 and W4 types in the QBOW and QBOE phases in the Northern Hemisphere are dominated by background atmospheric instabilities and winds.

3.3 Comparison between SH and NH

https://doi.org/10.5194/acp-2022-778
Preprint. Discussion started: 14 December 2022

Atmospheric Chemistry and Physics Discussions

Figure 8 shows the difference in mean background zonal winds between W3 and W4 events at the QBOW and QBOE phases in the Northern and Southern Hemispheres. Figures 8a and 8b show the difference between W3 and W4 in the Southern Hemisphere. Figure 8a shows that the mean background zonal wind of W3 at QBOW phase is weaker than that of QBOE phase on the whole, and the mean background zonal wind at ~50-70˚S and ~60-80 km (red dashed box) reaches ~8 m/s. The difference between ~20˚S-20˚N and ~50 km reaches ~35 m/s. The mean background zonal wind of W4 in the QBOW phase is stronger than that in the QBOE phase, and the difference between the mean background zonal wind at ~40-60˚S and ~50-70 km (red dashed box) is ~6 m/s. The difference between ~20˚S-20˚N and ~50 km reaches ~10 m/s (Figure 8b). We argue that the zonal winds of W3 in the Southern Hemisphere are stronger in the QBOE than in the QBOW, but with opposite temperature amplitudes, because the propagation and amplification of W3 in the Southern Hemisphere are affected by atmospheric intrinsic models. However, the zonal winds of W4 in the Southern Hemisphere are stronger than those of the QBOE in the QBOW, which is consistent with the structure of the temperature amplitude, suggesting that the propagation and amplification of W4 in the Southern Hemisphere are susceptible to atmospheric background variability.

Figures 8c and 8d show the difference between W3 and W4 in the

https://doi.org/10.5194/acp-2022-778
Preprint. Discussion started: 14 December 2022

Atmospheric Chemistry and Physics Discussions

Northern Hemisphere. Figure 8c shows that the mean background zonal wind of W3 in the QBOW phase is stronger than that of the QBOE phase as a whole, and the mean background zonal wind at ~50-70°N and ~60-80 km (red dashed box) reaches ~6 m/s. The difference between ~20°S-20°N and ~50 km reaches ~11 m/s; The difference between ~5-25°N and ~60 km reaches ~11 m/s. The mean background zonal wind of W4 in the QBOW phase is stronger than that in the QBOE phase, and the difference between the mean background zonal wind at ~40-60°N and ~50-70 km (red dashed box) is ~7 m/s. The difference between ~20°S-20°N and ~50 km reaches ~16 m/s (Figure 8d). We believe that the zonal winds of W3 and W4 in the northern hemisphere are stronger in the QBOW than in the QBOE, consistent with the temperature amplitude results because the propagation and amplification of W3 and W4 in the Northern Hemisphere are susceptible to changes in the atmospheric background.

Figure 9 shows the geopotential height (GPH) amplitudes derived from the MERRA2 data at 10 hPa for the Southern Hemisphere W3 and W4 events during the QBOW and QBOE phases, as well as the differences between the QBOW and QBOE phases. The red line region is the primary occurrence date of W3 and W4. Figure 9a shows the GPH amplitude of W3 in the QBOW phase, which reaches a maximum amplitude of ~20 m in the 15–30 days source region. The maximum amplitude at the QBOE phase is ~18 m (Figure 9b). As shown in Figure 9c, the difference of W3 in QBOW

https://doi.org/10.5194/acp-2022-778
Preprint. Discussion started: 14 December 2022

and QBOE phases (red dashed box) reaches a maximum of ~11 m. Figure 9d shows the GPH amplitude of W4 in the QBOW phase, which reaches ~9 m in the 15–30 days source region. The maximum amplitude at the QBOE phase is ~7 m (Figure 9e). As shown in Figure 9f, the difference between the QBOW and QBOE phases of W4 (red dashed box) reaches a maximum of ~3 m. We conclude that the source activity in the Southern Hemisphere of W3 and W4 in the QBOW phase provides stronger energy than in the QBOE phase to facilitate the propagation and amplification of W3 and W4 in the Southern Hemisphere.

Figure 10 shows the GPH amplitudes of the W3 and W4 events in the Northern Hemisphere during the QBOW and QBOE phases, as well as the difference between the QBOW and QBOE phases. The red line region is the primary occurrence date of W3 and W4. Figure 10a shows the GPH amplitude of W3 in the QBOW phase, which reaches ~12 m in the source region at 195-210 days. The maximum amplitude at the QBOE phase is ~11 m (Figure10b). As shown in Figure 10c, the difference between the QBOW and QBOE phases of W3 (red dashed box) reaches a maximum of ~3 m. Figure 10d shows the GPH amplitude of W4 in the QBOW phase, with a maximum amplitude of ~4 m in the source region from 195 to 210 days. The maximum amplitude at the QBOE phase is ~3 m (Figure 10e). As shown in Figure 10f, the difference between the QBOW and QBOE phases of W4 (red dashed box) reaches a maximum of ~2 m. We believe

https://doi.org/10.5194/acp-2022-778
Preprint. Discussion started: 14 December 2022

Atmospheric Chemistry and Physics Discussions

that the easy propagation and amplification of W3 and W4 in the Northern Hemisphere during the QBOW phase is because the source activity of W3 and W4 is stronger in the QBOW than in the QBOE, providing more energy.

4 Summary and Conclusions

We present the first extensive study of the differences between W3 and W4 in the QBOW and QBOE phases, identified from the analysis of the temperature and wind observations from 2003 to 2020 with SABER and MERRA-2. We first analyze the differences between the 2006/2007 QBOW and QBOE phases for W3 and W4, since 2006/2007 is representative of the entire range from 2003 to 2020. W3 and W4 events from 2003 to 2020 were identified using a two-dimensional least-squares fit. W4 was observed at ~30-40°(S/N) and ~67-73 km, while W3 was observed at ~30-40°S and ~79-85 km. W3 was observed at ~30-40°N and ~67-73 km. Our study covers events in both the Northern and Southern hemispheres and provides a comprehensive diagnostic analysis of their propagation and amplification in the QBOW and QBOE phases. The main findings of this study are summarized below:

1. The mean zonal wind amplitude at the equator is stronger in the QBOE than in the QBOW. Easterly wind amplitudes at 70˚(S/N) and ~70 km (in early January/middle July) were stronger in QBOE than in the QBOW phase. Westerly wind amplitudes at 70˚(S/N) and ~70 km (in early August/late February) were stronger in QBOW than in the QBOE phase.

https://doi.org/10.5194/acp-2022-778
Preprint. Discussion started: 14 December 2022

2. In 2006, the temperature spatial structure of the southern hemisphere W3 in the QBOE phase showed a bimodal structure with amplitudes of ~17 K and ~12 K at ~68 km and ~82 km, respectively, while the QBOW phase showed a unimodal structure with a maximum amplitude of ~14 K at ~82 km.

3. The mean temperature amplitudes of W3 and W4 in both hemispheres are stronger in the QBOW phase than in the QBOE phase. At the same time, their instabilities and background winds are stronger in the QBOW phase than in the QBOE phase, except W3 in the Southern Hemisphere.

4. Q2DW is more favorable for propagation in the summer hemisphere of the QBOW phase, where the mean flow instability and appropriate background winds in the mid-latitude between 40 km and 80 km considerably amplify planetary wave propagation. Moreover, the amplification of planetary waves via wave-means flow interactions can easily occur near their critical layer.

5. The source activity in the QBOW phase of W3 and W4 in both hemispheres is more likely to generate sufficient energy to facilitate the propagation and amplification of W3 and W4 in the QBOW phase than in the QBOE phase.

Overall, this study reveals a difference between the dynamics of mid-latitude westward planetary waves in the QBOW and QBOE phases.

https://doi.org/10.5194/acp-2022-778
Preprint. Discussion started: 14 December 2022

Atmospheric Chemistry and Physics Discussions

data availability. MERRA-2 data are available at http://disc.gsfc.nasa.gov. SABER data were downloaded from http://saber.gats-inc.com/data.php.

Code availability. Code is available at https://1drv.ms/f/s!AnW2rFlErpPchHIMgX-gOLZGpbXg.

Author contributions. LT carried out the data processing and analysis and wrote the manuscript. SYG, SYZ and DW contributed to reviewing the article.

Competing interests. The authors declare that they have no conflict of interest.

Acknowledgements. This work was performed in the framework of Space Physics Research (SPR). The authors thank NASA for free online access to the MERRA-2 temperature reanalysis.

Financial support. This research work was supported by the National Natural Science Foundation of China (41704153, 41874181, and 41831071).

https://doi.org/10.5194/acp-2022-778
Preprint. Discussion started: 14 December 2022

References

Baldwin, M. P., Gray, L. J., Dunkerton, T. J., Hamilton, K., Haynes, P. H., Randel, W. J., Holton, J. R., Alexander, M. J., Hirota, I., Horinouchi, T., Jones, D. B. A., Kinnersley, J. S., Marquardt, C., Sato, K., and Takahashi, M.: The quasi-biennial oscillation, Reviews of Geophysics, 39, 179-229, https://doi.org/10.1029/1999RG000073, 2001.

Chang, L. C., Palo, S. E., and Liu, H.-L.: Short-term variability in the migrating diurnal tide caused by interactions with the quasi 2 day wave, Journal of Geophysical Research: Atmospheres, 116, https://doi.org/10.1029/2010JD014996, 2011.

Coy, L., Wargan, K., Molod, A. M., McCarty, W. R., and Pawson, S.: Structure and Dynamics of the Quasi-Biennial Oscillation in MERRA-2, Journal of Climate, 29, 5339-5354, 10.1175/JCLI-D-15-0809.1, 2016.

Garfinkel, C. I., Shaw, T. A., Hartmann, D. L., and Waugh, D. W.: Does the Holton–Tan Mechanism Explain How the Quasi-Biennial Oscillation Modulates the Arctic Polar Vortex?, Journal of the Atmospheric Sciences, 69, 1713-1733, 10.1175/JAS-D-11-0209.1, 2012.

Gelaro, R., McCarty, W., Suárez, M. J., Todling, R., Molod, A., Takacs, L., Randles, C. A., Darmenov, A., Bosilovich, M. G., Reichle, R., Wargan, K., Coy, L., Cullather, R., Draper, C., Akella, S., Buchard, V., Conaty, A., da Silva, A. M., Gu, W., Kim, G.-K., Koster, R., Lucchesi, R., Merkova, D., Nielsen, J. E., Partyka, G., Pawson, S., Putman, W., Rienecker, M., Schubert, S. D., Sienkiewicz, M., and Zhao, B.: The Modern-Era Retrospective Analysis for Research and Applications, Version 2 (MERRA-2), Journal of Climate, 30, 5419-5454, 10.1175/JCLI-D-16-0758.1, 2017.

Gray, L. J., Crooks, S., Pascoe, C., Sparrow, S., and Palmer, M.: Solar and QBO Influences on the Timing of Stratospheric Sudden Warmings, Journal of the Atmospheric Sciences, 61, 2777-2796, 10.1175/JAS-3297.1, 2004.

Gray, W. M., Sheaffer, J. D., and Knaff, J. A.: Hypothesized mechanism for stratospheric QBO influence on ENSO variability, Geophysical Research Letters, 19, 107-110, https://doi.org/10.1029/91GL02950, 1992.

Gu, S.-Y., Dou, X., Pancheva, D., Yi, W., and Chen, T.: Investigation of the Abnormal Quasi 2-Day Wave Activities During the Sudden Stratospheric Warming Period of January 2006, Journal of Geophysical Research: Space Physics, 123, 6031-6041, https://doi.org/10.1029/2018JA025596, 2018.

Gu, S.-Y., Liu, H.-L., Pedatella, N. M., Dou, X., Li, T., and Chen, T.: The quasi 2 day wave activities during 2007 austral summer period as revealed by Whole Atmosphere Community Climate Model, Journal of Geophysical Research: Space Physics, 121, 2743-2754, https://doi.org/10.1002/2015JA022225, 2016.

Gu, S.-Y., Tang, L., Hou, X., Zhao, H., Teng, C.-K.-M., and Dou, X.: Quasi-Two-Day Waves in the Northern Hemisphere Observed by TIMED/SABER Measurements During 2002–2019, Journal of Geophysical Research: Space Physics, 126, e2020JA028877, https://doi.org/10.1029/2020JA028877, 2021.

Gu, S.-Y., Dou, X.-K., Yang, C.-Y., Jia, M., Huang, K.-M., Huang, C.-M., and Zhang, S.-D.: Climatology and Anomaly of the Quasi-Two-Day Wave Behaviors During 2003–2018 Austral Summer Periods, Journal of Geophysical Research: Space Physics, 124, 544-556, https://doi.org/10.1029/2018JA026047, 2019.

Holton, J. R. and Austin, J.: The Influence of the Equatorial QBO on Sudden Stratospheric Warmings,

https://doi.org/10.5194/acp-2022-778
Preprint. Discussion started: 14 December 2022

Atmospheric Chemistry and Physics
Discussions

Journal of Atmospheric Sciences, 48, 607-618, 10.1175/1520-0469(1991)048<0607:TIOTEQ>2.0.CO;2, 1991.

Holton, J. R. and Tan, H.-C.: The Influence of the Equatorial Quasi-Biennial Oscillation on the Global Circulation at 50 mb, Journal of Atmospheric Sciences, 37, 2200-2208, 10.1175/1520-0469(1980)037<2200:TIOTEQ>2.0.CO;2, 1980.

Hood, L. L., Redman, M. A., Johnson, W. L., and Galarneau, T. J.: Stratospheric Influences on the MJO-Induced Rossby Wave Train: Effects on Intraseasonal Climate, Journal of Climate, 33, 365-389, 10.1175/JCLI-D-18-0811.1, 2020.

Huang, Y. Y., Zhang, S. D., Yi, F., Huang, C. M., Huang, K. M., Gan, Q., and Gong, Y.: Global climatological variability of quasi-two-day waves revealed by TIMED/SABER observations, Ann. Geophys., 31, 1061-1075, 10.5194/angeo-31-1061-2013, 2013.

Iimura, H., Fritts, D. C., Lieberman, R. S., Janches, D., Mitchell, N. J., Franke, S. J., Singer, W., Hocking, W. K., Taylor, M. J., and Moffat-Griffin, T.: Climatology of quasi-2-day wave structure and variability at middle latitudes in the northern and southern hemispheres, Journal of Atmospheric and Solar-Terrestrial Physics, 221, 105690, https://doi.org/10.1016/j.jastp.2021.105690, 2021.

Jiang, J., Shi, J., and Huang, F.: Quasi-Biennial Variability of Indian Ocean Subtropical Mode Water Subduction Driven by Atmospheric Circulation Modes during the Argo Period, Journal of Climate, 35, 4085-4098, 10.1175/JCLI-D-21-0509.1, 2022.

Kumar, Karanam, Kishore, Subrahmanyam, Kandula, Venkata, Mathew, Sneha, Susan, and Koushik: Simultaneous observations of the quasi 2-day wave climatology over the low and equatorial latitudes in the mesosphere lower thermosphere, Climate dynamics: Observational, theoretical and computational research on the climate system, 51, 221-233, 2018.

Li, H., Pilch Kedzierski, R., and Matthes, K.: On the forcings of the unusual Quasi-Biennial Oscillation structure in February 2016, Atmos. Chem. Phys., 20, 6541-6561, 10.5194/acp-20-6541-2020, 2020.

Liu, G., England, S. L., and Janches, D.: Quasi Two-, Three-, and Six-Day Planetary-Scale Wave Oscillations in the Upper Atmosphere Observed by TIMED/SABER Over ~17 Years During 2002–2018, Journal of Geophysical Research: Space Physics, 124, 9462-9474, https://doi.org/10.1029/2019JA026918, 2019.

Liu, H. L., Talaat, E. R., Roble, R. G., Lieberman, R. S., Riggin, D. M., and Yee, J. H.: The 6.5-day wave and its seasonal variability in the middle and upper atmosphere, Journal of Geophysical Research: Atmospheres, 109, https://doi.org/10.1029/2004JD004795, 2004.

Liu, J., Zhang, D., Hao, Y., and Xiao, Z.: Multi-instrumental Observations of the Quasi-16-Day Variations From the Lower Thermosphere to the Topside Ionosphere in the Low-Latitude Eastern Asian Sector During the 2017 Sudden Stratospheric Warming Event, Journal of Geophysical Research: Space Physics, 125, e2019JA027505, https://doi.org/10.1029/2019JA027505, 2020.

Lu, H., Bracegirdle, T. J., Phillips, T., Bushell, A., and Gray, L.: Mechanisms for the Holton-Tan relationship and its decadal variation, Journal of Geophysical Research: Atmospheres, 119, 2811-2830, https://doi.org/10.1002/2013JD021352, 2014.

Lu, X., Wu, H., Chu, X., Oberheide, J., Mlynczak, M. G., and Russell Iii, J. M.: Quasi-Biennial Oscillation of Short-Period Planetary Waves and Polar Night Jet in Winter Antarctica Observed in SABER and MERRA-2 and Mechanism Study With a Quasi-Geostrophic Model, Geophysical Research Letters, 46, 13526-13534, https://doi.org/10.1029/2019GL084759, 2019.

Ma, T., Chen, W., Huangfu, J., Song, L., and Cai, Q.: The observed influence of the Quasi-Biennial Oscillation in the lower equatorial stratosphere on the East Asian winter monsoon during early

https://doi.org/10.5194/acp-2022-778
Preprint. Discussion started: 14 December 2022

boreal winter, International Journal of Climatology, n/a, https://doi.org/10.1002/joc.7192, 2021.

Ma, Z., Gong, Y., Zhang, S., Zhou, Q., Huang, C., Huang, K., Yu, Y., Li, G., Ning, B., and Li, C.: Responses of Quasi 2 Day Waves in the MLT Region to the 2013 SSW Revealed by a Meteor Radar Chain, Geophysical Research Letters, 44, 9142-9150, https://doi.org/10.1002/2017GL074597, 2017.

Marshall, A. G., Hendon, H. H., Son, S.-W., and Lim, Y.: Impact of the quasi-biennial oscillation on predictability of the Madden–Julian oscillation, Climate Dynamics, 49, 1365-1377, 10.1007/s00382-016-3392-0, 2017.

Martin, Z., Wang, S., Nie, J., and Sobel, A.: The Impact of the QBO on MJO Convection in Cloud-Resolving Simulations, Journal of the Atmospheric Sciences, 76, 669-688, 10.1175/JAS-D-18-0179.1, 2019.

McCormack, J. P., Coy, L., and Singer, W.: Intraseasonal and interannual variability of the quasi 2 day wave in the Northern Hemisphere summer mesosphere, Journal of Geophysical Research: Atmospheres, 119, 2928-2946, https://doi.org/10.1002/2013JD020199, 2014.

Naoe, H. and Shibata, K.: Equatorial quasi-biennial oscillation influence on northern winter extratropical circulation, Journal of Geophysical Research: Atmospheres, 115, https://doi.org/10.1029/2009JD012952, 2010.

Naujokat, B.: An Update of the Observed Quasi-Biennial Oscillation of the Stratospheric Winds over the Tropics, Journal of Atmospheric Sciences, 43, 1873-1877, 10.1175/1520-0469(1986)043<1873:AUOTOQ>2.0.CO;2, 1986.

Nishimoto, E. and Yoden, S.: Influence of the Stratospheric Quasi-Biennial Oscillation on the Madden–Julian Oscillation during Austral Summer, Journal of the Atmospheric Sciences, 74, 1105-1125, 10.1175/JAS-D-16-0205.1, 2017.

Pancheva, D., Mukhtarov, P., and Siskind, D. E.: Climatology of the quasi-2-day waves observed in the MLS/Aura measurements (2005–2014), Journal of Atmospheric and Solar-Terrestrial Physics, 171, 210-224, https://doi.org/10.1016/j.jastp.2017.05.002, 2018.

Pancheva, D., Mukhtarov, P., Siskind, D. E., and Smith, A. K.: Global distribution and variability of quasi 2 day waves based on the NOGAPS-ALPHA reanalysis model, Journal of Geophysical Research: Space Physics, 121, 11,422-411,449, https://doi.org/10.1002/2016JA023381, 2016.

Peña-Ortiz, C., Manzini, E., and Giorgetta, M. A.: Tropical Deep Convection Impact on Southern Winter Stationary Waves and Its Modulation by the Quasi-Biennial Oscillation, Journal of Climate, 32, 7453-7467, 10.1175/JCLI-D-18-0763.1, 2019.

Plumb, R. A.: Baroclinic Instability of the Summer Mesosphere: A Mechanism for the Quasi-Two-Day Wave?, Journal of Atmospheric Sciences, 40, 262-270, 10.1175/1520-0469(1983)040<0262:BIOTSM>2.0.CO;2, 1983.

Qin, Y., Gu, S.-Y., and Dou, X.: A New Mechanism for the Generation of Quasi-6-Day and Quasi-10-Day Waves During the 2019 Antarctic Sudden Stratospheric Warming, Journal of Geophysical Research: Atmospheres, 126, e2021JD035568, https://doi.org/10.1029/2021JD035568, 2021a.

Qin, Y., Gu, S.-Y., Dou, X., Teng, C.-K.-M., and Li, H.: On the Westward Quasi-8-Day Planetary Waves in the Middle Atmosphere During Arctic Sudden Stratospheric Warmings, Journal of Geophysical Research: Atmospheres, 126, e2021JD035071, https://doi.org/10.1029/2021JD035071, 2021b.

Reed, R. J., Campbell, W. J., Rasmussen, L. A., and Rogers, D. G.: Evidence of a downward-propagating, annual wind reversal in the equatorial stratosphere, Journal of Geophysical Research (1896-1977), 66, 813-818, https://doi.org/10.1029/JZ066i003p00813, 1961.

https://doi.org/10.5194/acp-2022-778
Preprint. Discussion started: 14 December 2022

Atmospheric Chemistry and Physics Discussions

Reid, K. J., King, A. D., Lane, T. P., and Hudson, D.: Tropical, Subtropical, and Extratropical Atmospheric Rivers in the Australian Region, Journal of Climate, 35, 2697-2708, 10.1175/JCLI-D-21-0606.1, 2022.

Remsberg, E. E., Marshall, B. T., Garcia-Comas, M., Krueger, D., Lingenfelser, G. S., Martin-Torres, J., Mlynczak, M. G., Russell III, J. M., Smith, A. K., Zhao, Y., Brown, C., Gordley, L. L., Lopez-Gonzalez, M. J., Lopez-Puertas, M., She, C.-Y., Taylor, M. J., and Thompson, R. E.: Assessment of the quality of the Version 1.07 temperature-versus-pressure profiles of the middle atmosphere from TIMED/SABER, Journal of Geophysical Research: Atmospheres, 113, https://doi.org/10.1029/2008JD010013, 2008.

Salby, M. L.: Rossby normal modes in nonuniform background configurations. Part I: simple fields, Journal of the Atmospheric Sciences, 38, 1803-1826, 10.1175/1520-0469(1981)038<1803:RNMINB>2.0.CO;2, 1981a.

Salby, M. L.: Rossby Normal Modes in Nonuniform Background Configurations. Part II. Equinox and Solstice Conditions, Journal of Atmospheric Sciences, 38, 1827-1840, 10.1175/1520-0469(1981)038<1827:RNMINB>2.0.CO;2, 1981b.

Son, S.-W., Lim, Y., Yoo, C., Hendon, H. H., and Kim, J.: Stratospheric Control of the Madden–Julian Oscillation, Journal of Climate, 30, 1909-1922, 10.1175/JCLI-D-16-0620.1, 2017.

Sun, L., Deser, C., Simpson, I., and Sigmond, M.: Uncertainty in the Winter Tropospheric Response to Arctic Sea Ice Loss: The Role of Stratospheric Polar Vortex Internal Variability, Journal of Climate, 35, 3109-3130, 10.1175/JCLI-D-21-0543.1, 2022.

Tang, L., Gu, S. Y., and Dou, X. K.: Eastward-propagating planetary waves in the polar middle atmosphere, Atmos. Chem. Phys., 21, 17495-17512, 10.5194/acp-21-17495-2021, 2021.

Tian, E. W., Su, H., Tian, B., and Jiang, J. H.: Interannual variations of water vapor in the tropical upper troposphere and the lower and middle stratosphere and their connections to ENSO and QBO, Atmos. Chem. Phys., 19, 9913-9926, 10.5194/acp-19-9913-2019, 2019.

Veryard, R. G. and Ebdon, R. A.: Fluctuations in tropical stratospheric winds, Meteorology Magazine, 125-143, 1961.

Xiong, J., Wan, W., Ding, F., Liu, L., Hu, L., and Yan, C.: Two Day Wave Traveling Westward With Wave Number 1 During the Sudden Stratospheric Warming in January 2017, Journal of Geophysical Research: Space Physics, 123, 3005-3013, https://doi.org/10.1002/2017JA025171, 2018.

Yamashita, Y., Akiyoshi, H., and Takahashi, M.: Dynamical response in the Northern Hemisphere midlatitude and high-latitude winter to the QBO simulated by CCSR/NIES CCM, Journal of Geophysical Research: Atmospheres, 116, https://doi.org/10.1029/2010JD015016, 2011.

Yamazaki, K., Nakamura, T., Ukita, J., and Hoshi, K.: A tropospheric pathway of the stratospheric quasi-biennial oscillation (QBO) impact on the boreal winter polar vortex, Atmos. Chem. Phys., 20, 5111-5127, 10.5194/acp-20-5111-2020, 2020.

Yoo, C. and Son, S.-W.: Modulation of the boreal wintertime Madden-Julian oscillation by the stratospheric quasi-biennial oscillation, Geophysical Research Letters, 43, 1392-1398, https://doi.org/10.1002/2016GL067762, 2016.

Zhang, R., Zhou, W., Tian, W., Zhang, Y., Liu, Z., and Cheung, P. K. Y.: Changes in the Relationship between ENSO and the Winter Arctic Stratospheric Polar Vortex in Recent Decades, Journal of Climate, 35, 5399-5414, 10.1175/JCLI-D-21-0924.1, 2022.

https://doi.org/10.5194/acp-2022-778
Preprint. Discussion started: 14 December 2022

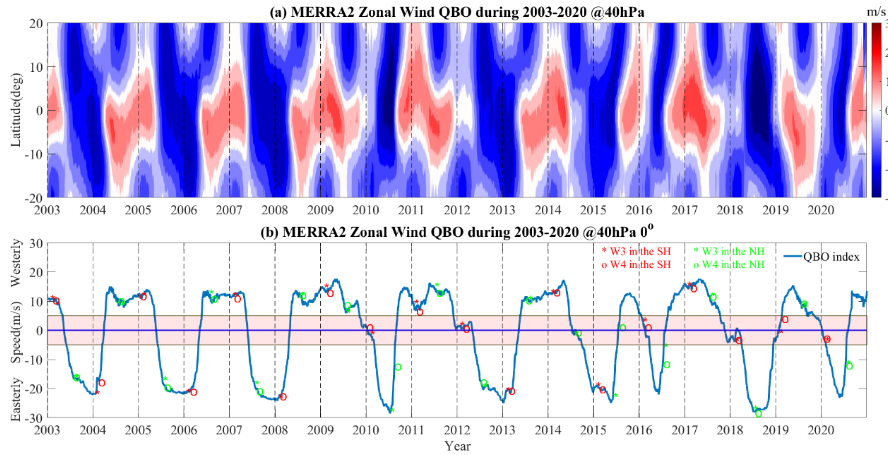

Figure 1. MERRA-2 zonal mean zonal wind between 20°S and 20°N at 40 hPa (1a) during 2003-2020. (1b) QBO index (blue line) at 0° and 40 hPa; Dots are the occurrence dates of the maximum amplitudes of W3 (*) and W4 (o). The red/green dots highlight SH/NH. The red-shaded region is the mean zonal wind at -5m/s to 5m/s (1b).

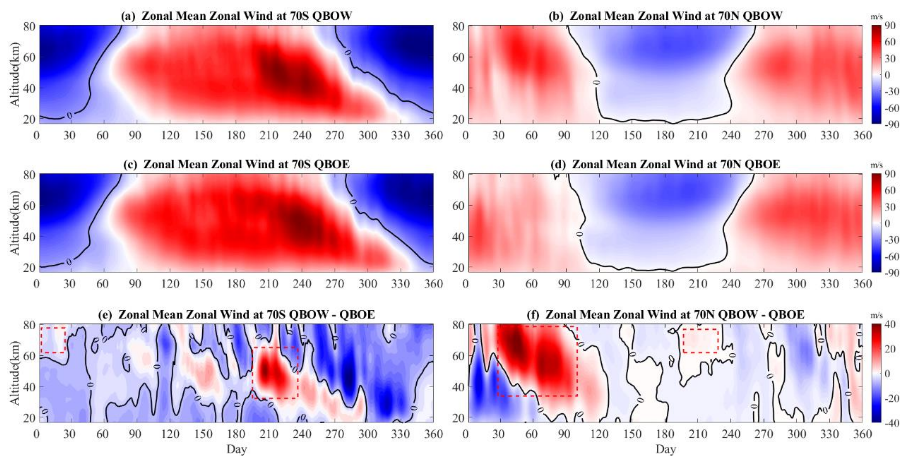

Figure 2. Seasonal variations of the zonal mean zonal wind amplitudes in QBOW and QBOE and differences of QBOW-QBOE during 2003-2020 for (a and c) MERRA-2 zonal mean wind in QBOW and QBOE at the 70S,

https://doi.org/10.5194/acp-2022-778
Preprint. Discussion started: 14 December 2022

Atmospheric Chemistry and Physics Discussions

(b and d) zonal mean wind in QBOW and QBOE at 70N, and (e and f) differences of zonal mean winds in QBOW to QBOE. The dashed red boxes in Figures 2e and 2f highlight the regions where the zonal mean wind enhancement is observed.

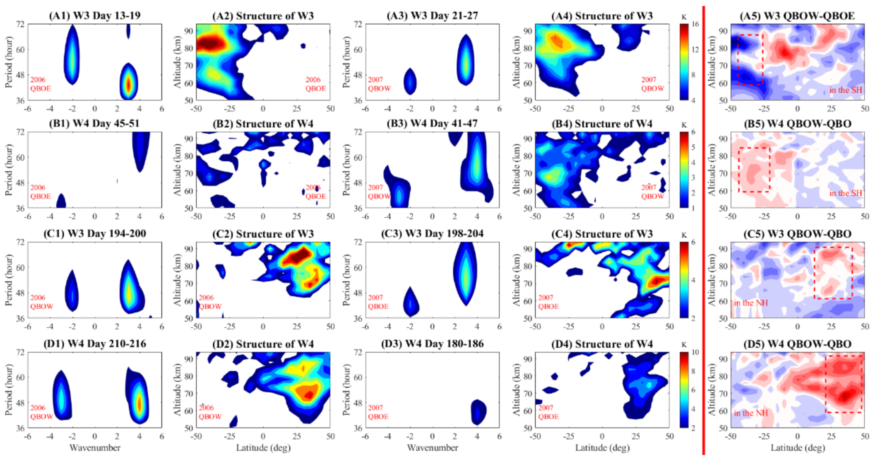

Figure 3. The (3A1, 3A3, 3B1, 3B3, 3C1, 3C3, 3D1, and 3D3) spectra and (3A2, 3A4, 3B2, 3B4, 3C2, 3C4, 3D2, and 3D4) structures of the W3 and W4 quasi-2-day wave events during 2006/2007 summer period. Differences of temperature amplitude in QBOW to QBOE (3A-D5). The 2006 SABER temperature observations during days 13–19 (3A1), days 45–51 (3B1), days 194-200 (3C1), and days 210-216 (3D1) are used; during 2007 days 21-27 (3A3), days 41-47 (3B3), days 198-204 (3C3), and days 180-186 (3D3) are used. Figures 3A1-3A2 and 3B1-3B2 are W3 and W4 of the 2006 summer QBOE phase; Figures 3A3-3A4 and 3B3-3B4 are W3 and W4 of the 2007 summer QBOW phase. Figures 3C1-3C2 and 3D1-3D2 are W3 and W4 of the 2006 summer QBOW phase; Figures 3C3-3C4

https://doi.org/10.5194/acp-2022-778
Preprint. Discussion started: 14 December 2022

Atmospheric Chemistry and Physics Discussions
Open Access
EGU

and 3D3-3D4 are W3 and W4 of the 2007 summer QBOE phase. The dashed red boxes in Figures 3A-D5 highlight the regions where the temperature amplitude enhancement is observed.

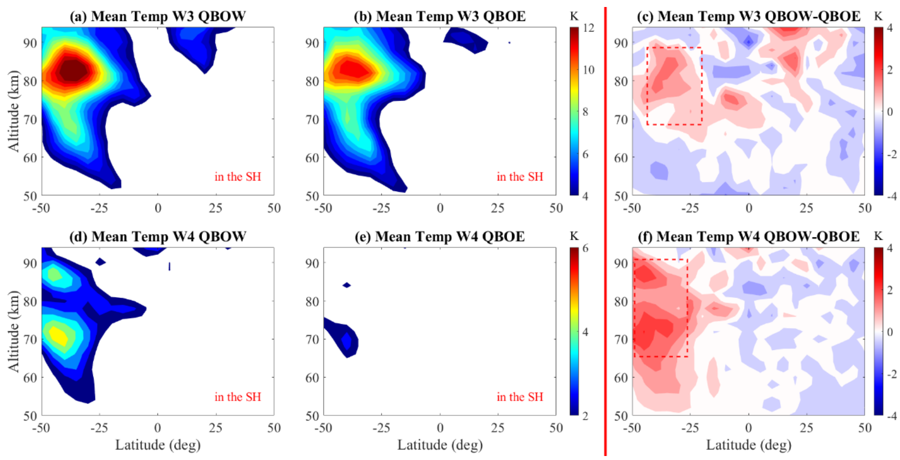

Figure 4. The spatial structure of the mean temperatures of the W3 and W4 Q2DWs during the Southern Hemisphere summer is captured in Figures 4a-4b and 4d-4e, respectively. The temperature amplitudes of the W3 and W4 events in the QBOW and QBOE were extracted from the SABER temperature data, respectively. Differences of temperature amplitude in QBOW to QBOE (4c, 4f). The dashed red box highlights the region where the observed enhancement of the temperature amplitude is observed.

https://doi.org/10.5194/acp-2022-778
Preprint. Discussion started: 14 December 2022

Atmospheric Chemistry and Physics
Discussions
Open Access
EGU

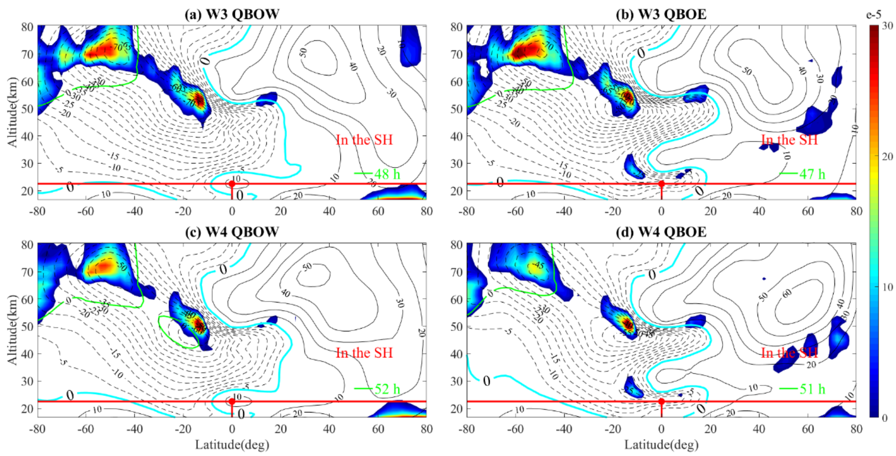

Figure 5. Diagnostic analysis results of the QBOW (Figures 5a and 5c) and QBOE (Figures 5b and 5d) quasi-two-day waves for W3 (Figures 5a and 5b) and W4 (Figures 5c and 5d). The blue-shaded region is the instability, the red line is the QBO phase, the cyan line is the null wind, and the green line is the critical layer. The green line shows the critical layer E1 with the mean period.

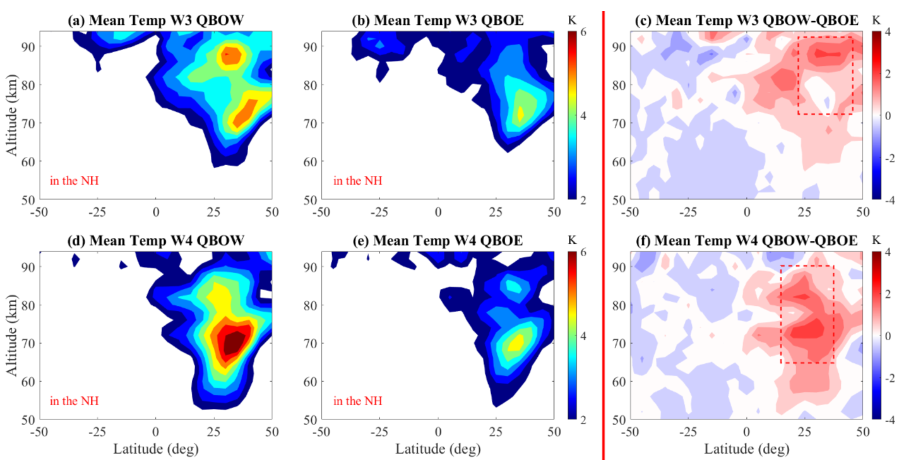

Figure 6. Same as Figure 4 but for W3 and W4 during the Northern Hemisphere summer.

https://doi.org/10.5194/acp-2022-778
Preprint. Discussion started: 14 December 2022

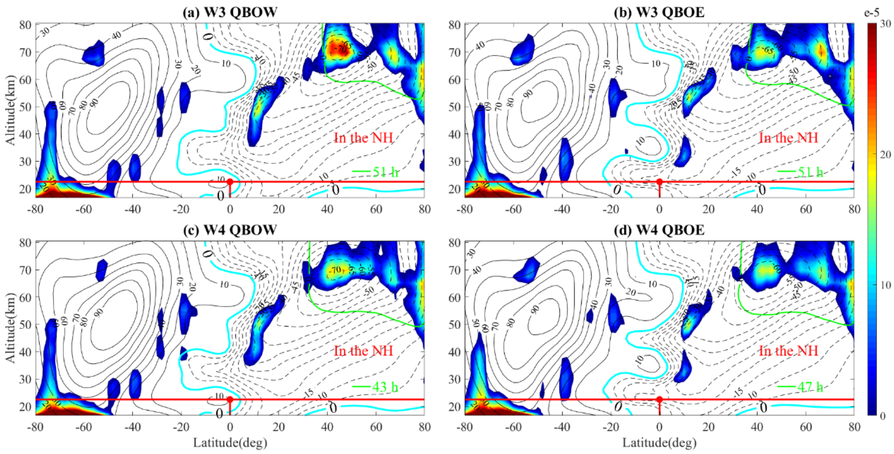

Figure 7. Same as Figure 5 but for W3 and W4 during the Northern Hemisphere summer.

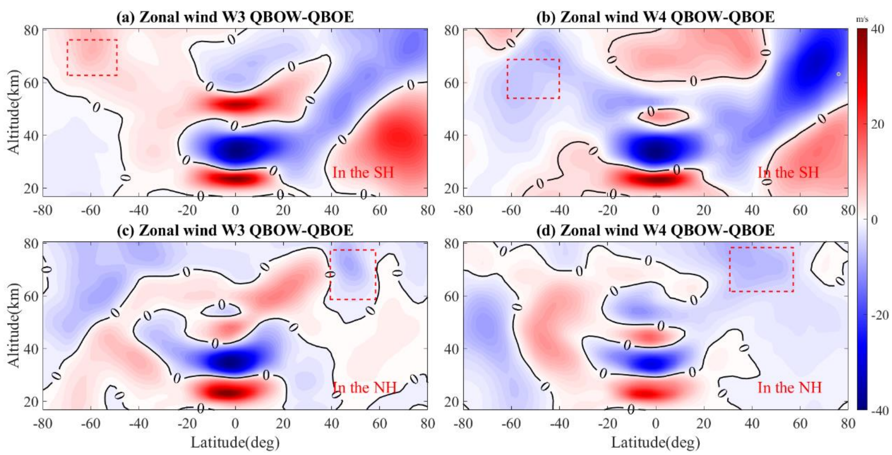

Figure 8. Differences in the zonal mean winds from QBOW to QBOE in SH and NH. (8a, 8c) W3 and (8b, 8d) W4 amplitudes, respectively.

https://doi.org/10.5194/acp-2022-778
Preprint. Discussion started: 14 December 2022

Atmospheric Chemistry and Physics
Discussions

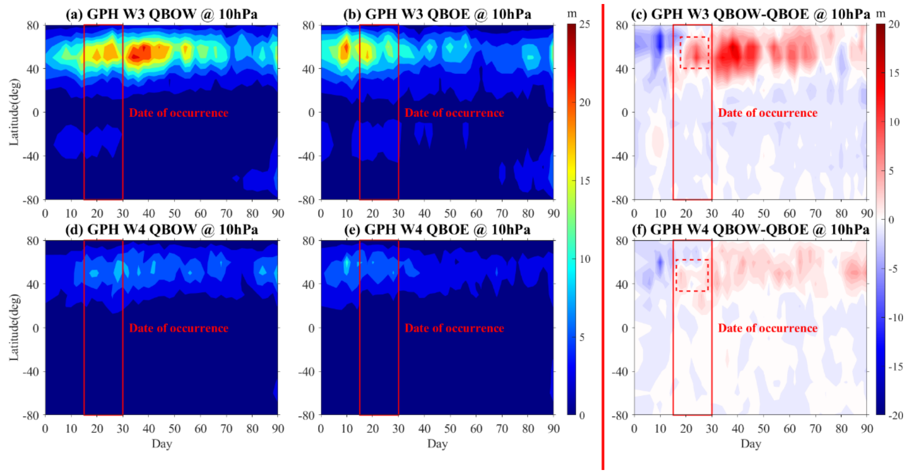

Figure 9. Temporal variations of GPH of the QBOW (Figures 9a and 9d) and QBOE (Figures 9b and 9e) for W3 (Figures 9a and 9b) and W4 (Figures 9d and 9e) during Southern Hemisphere summer. Regions enclosed by solid red lines are characterized by the date of major occurrence of W3 and W4. The dashed red box highlights the region where an enhancement of the observed GPH amplitude is observed.

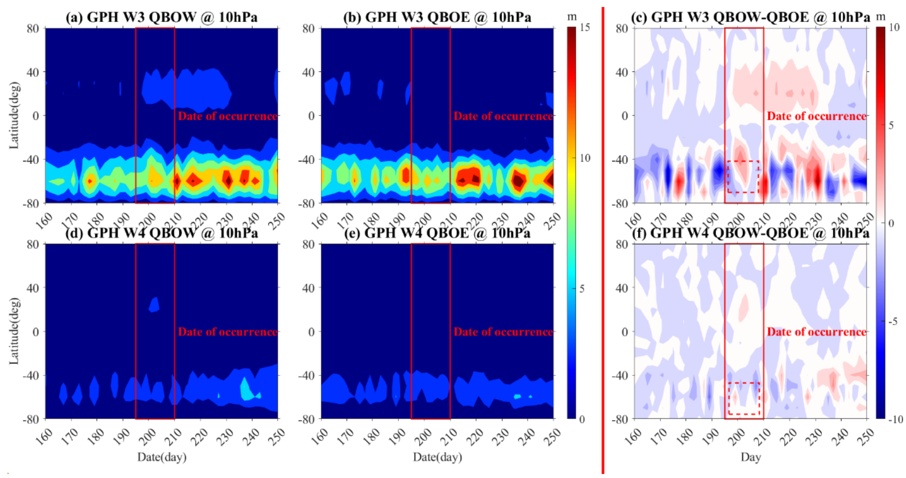

Figure 10. Same as Figure 9 but for W3 and W4 during the Northern Hemisphere summer.